RESEARCH ARTICLE OPEN ACCESS

# An Optimal Design of the Eddy Current Non-Destructive Testing Sensor for Special Geometries of Conducting Materials

Abderraouf Bouloudenine*,**, Mohamed El Hadi Latreche*,**, Abdallah Belounis*,** and Nacir Boutra*,**.

*Electrical Engineering laboratory of Constantine, Campus Ahmed Hammani, University of Constantine 1, Way of Ain El-Bey 25000, Constantine, Algeria.
**Inductique Research Network - ATRST – Algeria.

**ABSTRACT**
Non-destructive eddy current testing technic is more and more exploited because it is quick and none contacting into the inspected materials. In order to increase the signal sensing of non-destructive eddy current testing sensors, we are going to propose an optimal design of coil sensor. This optimization needs to construct a tilted cross section coil according to the tested piece geometry. In our simulations, the finite-element method has been exploited for geometrical and physical modelling. For the extraction of our results, a finite-element method code was built in COMSOL with MATLAB. In this paper we compare the tilted cross section coil with a rectangular cross section coil. To obtain the influence of the coil shape on the sensitivity of eddy current sensor, we use the relationship between the impedance changes and the sensor displacement in the two cases of comparison.

***Keywords*** - non-destructive eddy current testing, crack detection, impedance change, finite-element method, design optimization.

## I. INTRODUCTION

The development of non-destructive tools for the inspection of such material is in strong demand for many practical applications. Various methods based on ultrasonic, thermography and electromagnetic technics [1-3]. In order to improve manufacturing quality and ensure public safety, components and structures are commonly inspected for early detection of defects or faults which may reduce their structural integrity. Nondestructive testing (NDT) and evaluation technics present the advantage of leaving the specimens which are undamaged after inspection [4]. Advanced research activity on NDT like in energy production, transportation, work piece manufacturing etc has been motivated by the need of precise evaluation of cracks and flaws for the assessment of the expected life of mechanical components [5].

Eddy current non-destructive testing (EC-NDT) is used which is a very effective and convenient way to nondestructively evaluate a metallic surface for cracks and other defects. Furthermore eddy Current Testing is a fast, reliable, and cost effective non-destructive testing method for inspecting plate, round and irregularly shaped conductive materials [3,6]. EC-NDT is based on considering the impact of eddy currents and on the usage of different excitation coils and sensors for measuring magnetic flux density or impedance change [1,4,7-9]. Eddy-current inspection for non-destructive evaluation has traditionally been investigated in terms of coil impedance signals. In the presence of defects which act as a high resistance of barrier, the eddy-current flow is perturbed. As a result of this defect, a "leakage" magnetic field is produced. Such field perturbations are usually detected as an impedance change in the exciting coil [5].

The EC-NDT signal is strongly related to the geometrical shape of the coil, i.e. the size, shape, and positioning of the coil. In EC-NDT applications, such as crack detection, the probe coil is usually having a circular shape and located above the piece of conducting material. The purpose of this paper is to find a better geometry of sensor that has more sensitivity when a crack appears in a conductive piece, on the basis of NDT with eddy currents. Tilted cross section (TCS) air cored coil is a new sensor's coil for EC-NDT proposed in this work for detection of cracks in pieces that have a shape as show in (Fig.1) Both of air cored circular sensor and tilted air cored sensor will be compared for testing the behavior of TCS sensor sensitivity.

To determine an optimal eddy current coil design, finite-elements method (FEM) analyses were carried out using the simulation software COMSOL with MATLAB. We have validated this design by using the benchmark problems TEAM (Testing Electro-magnetic Analysis Methods) Workshop 15-1 [8], a 3D electromagnetic formulation has been used for the resolution.

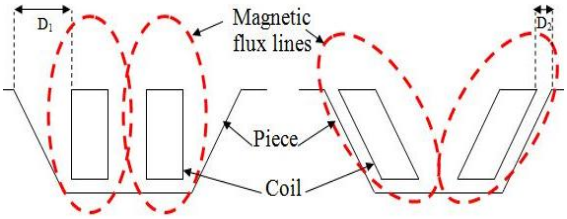


**Fig.1.** Design of the sensor's coil and the piece used in 2D. (a) With rectangular cross section coil. (b) With tilted cross section air cored coil.

## II. GEOMETRY PROBLEM

### 1.1. TEST PIECE

The test piece and crack have the same physical properties and geometric parameters which were used in benchmark problems TEAM Workshop 15-1[8], but in this work we make a modified piece by taking some changes in the plate. These changes are a deformation which has a depth $d_2 = 6.2\,mm$, length $l_2 = 90\,mm$ and width $w_2 = 28.8\,mm$, $w_3 = 20.8\,mm$. The tested piece with marked dimensions is shown in (Fig.2) Piece thickness is $c = 12.22\,mm$ with dimensions $l_1 = 100\,mm$ in the length and $w_2 = 50\,mm$ in the width. From (Fig.2 (a)) we can see that the two longitudinal boundaries of deformation are tilted by an angle α from the vertical plan, in direct sense for the right boundary and vice versa direction for the left boundary. We let the two transversal boundaries in vertical state.

Cracks positions are located as follow: In the first case (C1) the crack situated in the middle of piece, exactly at $h_1 = 0.056\,mm$ below the lower plate deformation surface. The second (C2), the third (C3) and the fourth (C4) cases of crack to be found in the right of the inner lateral deformation surface with $h_1 = 0.056\,mm$, and with $h_2 = 6.256\,mm$, $h_3 = 3.075\,mm$, $h_4 = 1.025\,mm$ low from the top surface plate. The crack has a depth $d = 0.5\,mm$, length $l = 12.6\,mm$ and width $w = 0.28\,mm$ [8]. The presence of the flaw is modeled by a change in the conductivity.

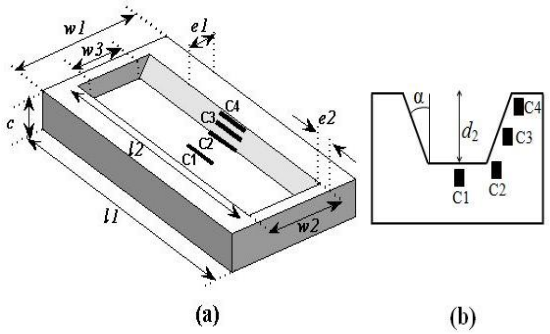


**Fig.2.** (a) 3D test piece with cracks positions. (b) Transversal cross section test piece with cracks positions.

### 1.2. SENSORS

In fact there are many designs of EC-NDT sensors, it may consist of ferrite or air core coil probes. These types of sensors usually are placed above a planar piece, inside or outside a tubular piece.

Two air cored sensors were employed in this paper, the first sensor (Fig.3 (a)) is modeled as a cylindrical cavity of rectangular cross section (RCS) with inner radius $R_1 = 6.15\,mm$, outer radius $R_2 = 12.4\,mm$ and height $h = 6.15\,mm$ [8]. The second is a new exciting sensor, it is obtained by the tilting of the cross section with an angle α, after we revolve the cross section with an angle equal to 360° (Fig.3 (b)), we get a TCS air cored coil. The bottom inner radius is $R_{bi} = 6.15\,mm$, the bottom outside radius $R_{bo} = 12.4\,mm$ and the height $h = 6.15\,mm$ . The top inner radius is $R_{ti} = 8.15\,mm$ and the top outside radius $R_{to} = 14.4\,mm$.

We can calculate the TCS angle from the following relation $\alpha = atan[\frac{(R_{ti} - R_{bi})}{h}]$, so in our simulation we find $\alpha_1 = 0°$(for the rectangular cross section coil), $\alpha_2 = 33.04°$ (for the tilted cross section coil).

Both sensors are supplied with a sinusoidal current of 6.15 $(A)$ and frequency of 900 $(Hz)$. The distance between the coil and the test piece is $lift\_off = 0.88\,mm$ above the plate.

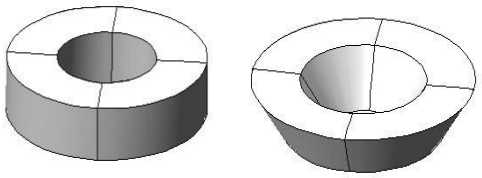


**Fig.3.** The used coils. (a) With rectangular cross section (RCS). (b)With tilted cross section (TCS).

## III. FORMULATION

### 1.3. EQUATIONS

In ECT, the problem concerns the determination of the probe impedance. The real (R) and imaginary (X) parts of the probe impedance are determined by using the power losses $(P_j)$ and the magnetic energy $(W_m)$, respectively. Both are deduced from the FEM results[8,9].

$$X = \omega \cdot \frac{\iiint_{espace} \mu . H^2 dv}{I^2} \quad (1)$$

$$R = \frac{\iiint_{espace} \frac{1}{\sigma} J^2 dv}{I^2} \quad (2)$$

Where $B, H, J, I, v, \sigma, \mu, \omega$ : the magnetic flux density, the magnetic field intensity, the current density, the current intensity, the volume, the electrical conductivity, the magnetic permeability and the angular frequency respectively.

The penetration depth of eddy current in the test piece can be calculated by $\delta = \frac{1}{\sqrt{\pi\mu\sigma f}}$ .Where f = 900 (Hz) is the excitation frequency, σ = 30,6e6 (S/m) is the electrical conductivity, and μr = 1 is the relative permeability of the material under inspection.

According to the conductivity and permeability of piece and the excitation frequency, the skin depth is 3 mm in the test piece. Therefore, the skin depth is certainly bigger than the crack depth. In order to set the current flowing within the coil as a point by point vector tangent to the coil itself, we used the direction cosine trigonometric formulation.

We have:

$$J = \frac{N.I}{h.(r2-r1)} \quad (3)$$

With N is the coil number of turns, $r1$ and $r2$ are the bottom inner radius and the bottom outer radius of the coil. h is the height of the coil.

The J vector is then expressed in the (x, y, z) coordinate system by the following formula:

$$J = [\frac{\|J_0\|.y}{\sqrt{x^2+y^2}} \ , \frac{-\|J_0\|.x}{\sqrt{x^2+y^2}} \ , 0 ] \quad (4)$$

$$\mathrm{I} = \mathrm{I}_{max} \cos(\omega.\mathrm{t}) \quad (5)$$

### 1.4. FINITE ELEMENT METHOD

The FEM program was written in MATLAB with conjunction with the commercial FEM simulation package COMSOL MULTIPHYSICS. Four regions are formed according to the problem geometry. The first element is the air domain, the second element is the tested piece, the third is the crack and the last one can be a circular air-core coil or TCS air-core coil. The coil displacement increases from -29 to 29 mm, with a step of 1mm for each simulation. The FEM was based on a discrete domain which has a number of elements. Mesh was generated with tetrahedral elements. In this study, our phenomenon is governed by the following equation:

$$(j\omega\sigma - \omega^2\varepsilon_0\varepsilon_r)\vec{A} + \vec{\nabla} \wedge \left(\mu_0{}^{-1}\mu_r{}^{-1}\vec{\nabla} \wedge \vec{A}\right) = \vec{J} \quad (6)$$

Where: $\varepsilon_0, \varepsilon_r, \mu_0, \mu_r$ are the void's dielectric constant, the electrical relative permittivity, the void's magnetic constant and the relative magnetic permeability.

We set the boundary conditions as follows: Magnetic insulation $\left(\vec{n} \wedge \vec{A}\right) = \vec{0}$, for the air subdomain. Regarding boundaries of plate and the coil, the continuity are insured by:

$$\vec{n} \wedge \left(\frac{1}{\mu}\vec{H_1} - \vec{H_2}\right) = \vec{0}.$$

## IV. RESULTS AND DISCUSSION

### 1.5. MAGNETIC FLUX AND EDDY CURRENT DISTRIBUTION

We have studied two types of the EC-NDT sensor. From (Fig.4) and (Fig.5) we can remark that the cross-section shape of coil has essential influence which is mainly relative to the distribution of the magnetic flux and eddy current density. Under the same condition, we find that the magnetic flux density is very important around the crack in the case of the TCS coil by contribution in the RCS coil, the magnetic flux density is poorer. In (Fig.5) we uncover the same behavior for the eddy current density. Where the cross section coil is rectangle we find that the eddy current density is lower but with the TCS coil we find a strong density.

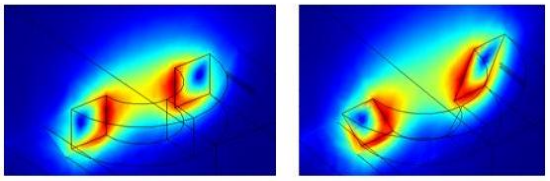

(a) (b)

**Fig.4.** Slice of the magnetic flux distribution. (a) For the rectangular cross section coil. (b) For the tilted cross section coil.

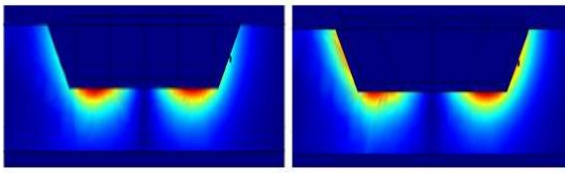

(a) (b)

**Fig.5.** Slice of the eddy current density. (a) With rectangular cross section coil. (b) With tilted cross section coil.

### 1.6. IMPEDANCE CHANGES

The sensor has been moved over the specimen with a distance of a 1 *mm* step-by-step along x axes. The impedance change is because of the presence of the flaw. The impedance values are calculated twice: with and without the crack. The difference of these two values was the impedance change. The plotted values are the impedance change due to the crack as a function of displacement.

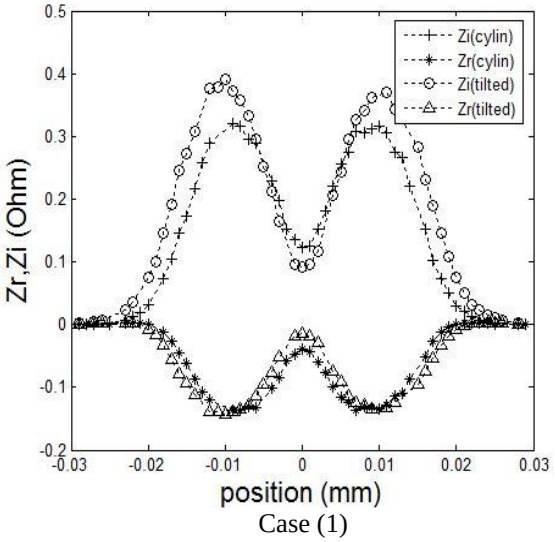


Case (1)

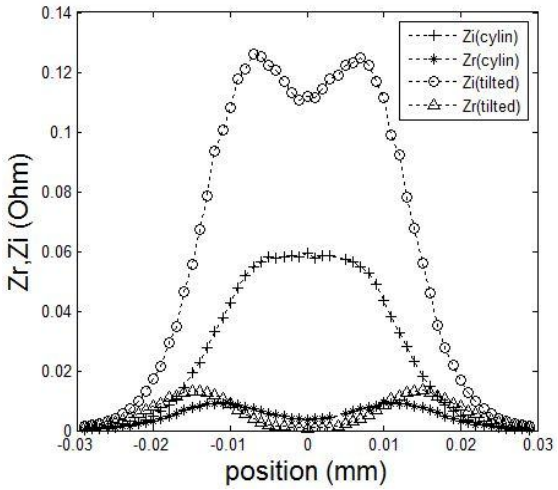

Case (2)

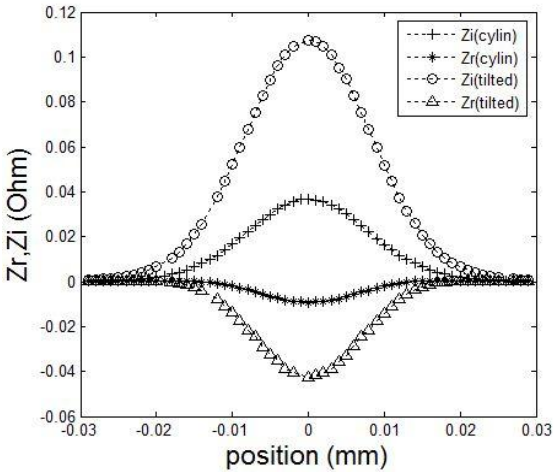

Case (3)

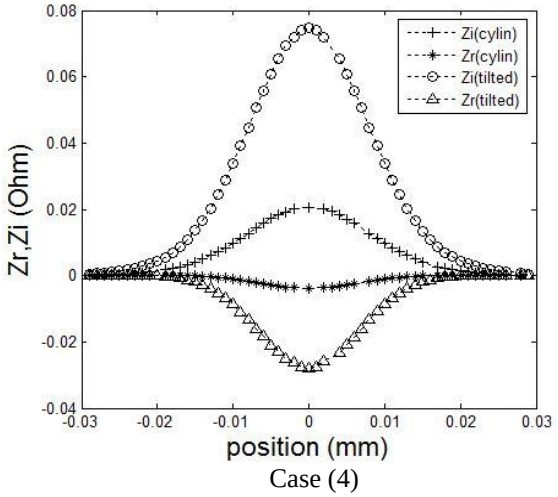

Case (4)

**Fig.6.** The real ($Z_r$) and imaginary ($Z_i$) parts of the probe impedance changes as function of displacement with four position of defect.

The impedance change obtained in four cases of defect positions as shown in (Fig.2) In every case the piece was tested by using the cylindrical excitation coil with RCS than it was tested again by using the excitation coil with TCS.

In the first case (Fig.6 (Case1)) when a probe was displaced above the crack, the obtained signal shows two symmetrical peaks that are located on each side of the crack. In the second case (Fig.6 (Case2)) when a crack position located beside the edge which meets the intern bottom surface connected with intern lateral surface of piece, from the cylindrical coil the obtained signal shows one flat arc that is located on the crack. But from the TCS coil, the signal obtained shows two peaks that are located on each side of the crack. In the third case (Fig.6 (Case3)) when a crack position located in the middle of lateral surface of piece, the obtained signal shows one peak that is located on the crack center. In the fourth case (Fig.6 (Case 4)) when a crack position located in the top of lateral surface of piece, the obtained signal shows one peak that is located on the crack center.

From (Fig.6) we can see too that the magnitudes of the real parts and the imaginary parts of impedance change obtained by the TCS coil are important by contributing with the RCS coil. According to the signal of the first, the third and the fourth cases, the imaginary parts of impedance change are positive while the real part is negative. But in the second case the real and the imaginary parts are positive.

### 1.7. COMPARISON BETWEEN THE IMPEDANCE CHANGES PERCENTAGE OF THE TWO TYPES OF SENSORS

In (Fig.7), the results are presented in terms with the importance of the impedance changes for the two sensor's types and for all previous positions of crack.

For the imaginary parts of the probe impedance changes (Fig.7 (a)) we get the following percentages: with RCS sensor 82.08%, 47.04%, 34% and 27.55% by contributing the TCS sensor.

For the imaginary parts of the probe impedance changes (Fig.7 (b)) we get the following percentages: with RCS sensor 98.35%, 68.90%, 21.93% and 13.94% by contributing the TCS sensor.

So we can remark that the sensitivity fitness of the TCS sensor is more than the sensitivity fitness of the RCS in all positions.

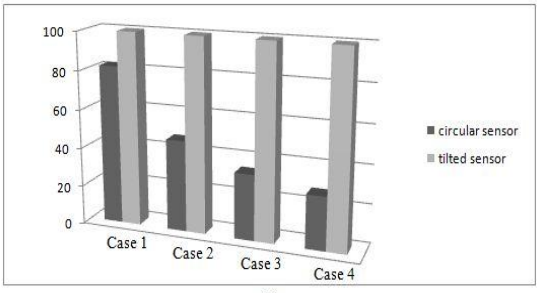

(a)

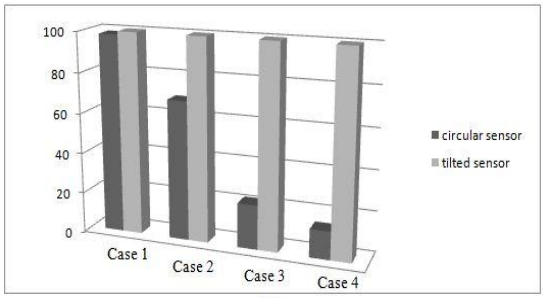


**Fig.7.** Impedance change percentage of the two sensors used. (a) The imaginary parts. (b) The real parts.

## V. CONCLUSION

In this paper we find that the cross-section shape has essential influence on the properties of eddy current testing sensor due to the influence of the coil shape on the distribution of the magnetic field. The tilted cross section sensor is a new non-destructive eddy current testing sensor, it was designed for the detection of crack in a spatial geometries of conducting pieces. For the inspection of crack in this type of geometries it appears that the tilted sensor is much more efficient than the rectangular cross section air-cored sensor.

## REFERENCES

[1] W. Yin, P.J. Withers, U. Sharma and J.A. Peyton, *Noncontact Characterization of Carbone-Fiber-Reinforced Plastics Using Multifrequency Eddy Current Sensors*, *IEEE Transactions on Instrumentation and measurement. 58(3),* 2009, 738-743.

[2] P. Vaaraet, J. Leiononen, *Technology Survey on NDT of Carbon-fiber Composites* ( Kemi-Tornio University of Applied Sciences: Finland, 2012).

[3] A. Zaoui, H, Menana, M. Feliachi, G Berthiau, *Inverse Problem in Nondestructive Testing Using Arrayed Eddy Current Sensors*. *Sensors. 10 (9),* 2010, 8696-8704.

[4] M. Cacciola, S. Calcagno, G. Megali, F.C. Morabito, D. Pellicanó, M. Versaci, *FEA Design and Misfit Minimization for In-Depth Flaw Characterization in Metallic Plates with Eddy Current Nondestructive Testing*. *IEEE Transactions on Magnitics. 45(3)* 2009, 1506-1509.

[5] T. Dogaru, S.T. Smith, *Giant Magnetoresistance-Based Eddy-Current Sensor*. *IEEE Transactions on Magnitics. 37(5),* 2001, 3831-3838.

[6] T. Griesbach, M.C Wurz, L. Rissing, *Modular Eddy Current Micro Sensor. IEEE Transactions on Magnetics. 47(10),* 2011, 3760-3763.

[7] T.P Teodoulidis, *Model of Ferrite-cored Probes for Eddy Current Nondestructive Evaluation*. *Journal of Applied physics. 93(5)* 2003, 3071-3078.

[8] L. Santandréa, Y. Le Bihan, *Using COMSOL-Multiphysics in an Eddy Current Non-Destructive Testing Context, Proc of the COMSOL Conference 2010, Paris, France.*

[9] M. Bensetti, Y. Choua, L. Santandréa,Y. Le Bihan, C. Marchand, *Adaptive Mesh Refinement and Probe signal Calculation in Eddy Current NDT Complementary Formulation*. *IEEE Transactions on Magenetics. 44(6),* 2008, 1646-1649.